Calcium mobilization stimulates *Dictyostelium discoideum* shear-flow-induced cell motility

Sébastien Fache[1,*], Jérémie Dalous[1], Mads Engelund[2], Christian Hansen[2], François Chamaraux[1], Bertrand Fourcade[1], Michel Satre[3], Peter Devreotes[4] and Franz Bruckert[3,5]

[1]Structures et Propriétés des Architectures Moléculaires (UMR 5919 CNRS), Département de Recherche Fondamentale sur la Matière Condensée, CEA-Grenoble, DRFMC/SI3M, 17 rue des Martyrs, 38054 Grenoble Cedex 09, France
[2]Image Analysis & Computer Graphics, Informatics and Mathematical Modelling, Technical University of Denmark, Richard Petersens Plads, Building 321, DK-2800 Kgs. Lyngby, Denmark
[3]Laboratoire de Biochimie et Biophysique des Systèmes Intégrés (UMR 5092 CNRS), Département Réponse et Dynamique Cellulaires, CEA-Grenoble, DRDC/BBSI, 17 rue des Martyrs, 38054 Grenoble Cedex 09, France
[4]Johns Hopkins University, School of Medicine, 725 N. Wolfe St., 114 WBSB, Baltimore, MD 21205, USA
[5]Laboratoire des Matériaux et Génie des Procédés, ENS de Physique de Grenoble, Domaine Universitaire, 38402 Saint-Martin d'Hères, France
*Author for correspondence (e-mail: fbruckert@cea.fr)

Accepted 27 April 2005
Journal of Cell Science 118, 3445-3457 Published by The Company of Biologists 2005
doi:10.1242/jcs.02461

Summary

Application of hydrodynamic mild shear stress to adherent *Dictyostelium discoideum* vegetative cells triggers active actin cytoskeleton remodeling resulting in net cell movement along the flow. The average cell speed is strongly stimulated by external calcium (Ca^{2+}, $K_{50\%}$=22 μM), but the directionality of the movement is almost unaffected. This calcium concentration is ten times higher than the one promoting cell adhesion to glass surfaces ($K_{50\%}$=2 μM). Addition of the calcium chelator EGTA or the Ca^{2+}-channel blocker gadolinium (Gd^{3+}) transiently stops cell movement. Monitoring the evolution of cell-surface contact area with time reveals that calcium stimulates cell speed by increasing the amplitude of both protrusion and retraction events at the cell edge, but not the frequency. As a consequence, with saturating external calcium concentrations, cells are sensitive to very low shear forces (20 pN; σ=0.1 Pa). Moreover, a null-mutant lacking the unique Gβ subunit does not respond to external Ca^{2+} changes ($K_{50\%}$>1000 μM), although the directionality of the movement is comparable with that of wild-type cells. Furthermore, cells lacking the inositol 1,4,5-trisphosphate receptor (IP_3-receptor) exhibit a markedly reduced Ca^{2+} sensitivity. Thus, calcium release from internal stores and calcium entry through the plasma membrane modulate cell speed in response to shear stress.

Supplementary material available online at
http://jcs.biologists.org/cgi/content/full/118/15/3445/DC1

Key words: Calcium, Heterotrimeric G proteins, Motility, Hydrodynamic flow, Mechanosensitivity, *Dictyostelium discoideum*

Introduction

Amoeboid motility is a widespread cell propulsive mechanism involving a combination of protrusive and retractive activity (Bailly and Condeelis, 2002; Friedl et al., 2001). The motor force for protrusion is the actin dendritic polymerization underneath the plasma membrane (Borisy and Svitkina, 2000) while that for retraction is provided by myosin-2-mediated contraction of actin filaments (Clow and McNally, 1999). Two different protein machineries can therefore be recruited at the edges of the cell-substrate adhesion surface ('adhesive belt'), with opposite mechanical effects.

At the molecular level, dendritic actin polymerization is controlled by small G proteins of the Rac/Cdc42 subfamily, which activate the Arp2/3 nucleator complex through WASP or VASP adaptor molecules (Krause et al., 2003; Welch and Mullins, 2002). Members of the myosin 1 family are also recruited and activated at the leading edge (Fukui et al., 1989). Small G proteins of the Rho subfamily stimulate growth of actin bundles and myosin 2 binding to actin through formin and Rho kinase (ROCK) activation (Gasteier et al., 2003). Efficient actin polymerization also requires barbed-end capping and uncapping activity (Carlier and Pantaloni, 1997; Pollard and Borisy, 2003) and the presence of profilin and cofilin to speed up the actin polymerization-depolymerization cycle (DesMarais et al., 2002; Wolven et al., 2000). The activity of many actin-binding proteins is regulated by phosphatidylinositol 4,5-bisphosphate (PIP_2), whose turnover is very active at the leading edge (Sakisaka et al., 1997). In particular, gelsolin, an actin filament-severing and barbed end-capping molecule, binds to PIP_2 and is released from the plasma membrane by micromolar concentrations of Ca^{2+} (Lin et al., 1997).

Recently, we have shown that application of hydrodynamic shear stress to *Dictyostelium discoideum* cells adhering to a flat glass surface triggers their movement in the direction of the flow (Décavé et al., 2003). Directionality of the movement requires the formation of a phosphatidylinositol 3,4,5-trisphosphate (PIP_3) gradient through phosphoinositide 3-kinase (PI3K) activity. Since forces applied to the cell are lower or comparable with the ones internally exerted by the cell during random motility or chemotaxis, it is likely that mechanosensitivity is part of a physiological mechanism controlling the local movement of

Journal of Cell Science

Journal of Cell Science

cell edges. Shear-flow-induced cell motility would therefore result from biasing the stress balance within the cell.

In this paper, we examine the role of calcium and heterotrimeric G proteins, two ubiquitous players of signaling pathways, in shear stress-induced motility. During chemotaxis, heterotrimeric G proteins play an essential role in determining the direction of cell movement (directional sensing) (Devreotes and Janetopoulos, 2003; Wu et al., 1995), whereas calcium entry through plasma membrane channels is associated with uropod contraction phases (Nebl and Fisher, 1997; Yumura et al., 1996). Here we show that the presence of external calcium entry and calcium release from internal stores stimulate the amplitude of cell protrusions and retractions in contact with the substrate. During shear-flow-induced motility, these calcium fluxes stimulate cell speed, but marginally affect cell directionality. Using knockout mutants, we show that heterotrimeric G proteins are also involved in the control of cell speed, but not cell direction, probably through the activation of phospholipase C and the IP_3-receptor.

Materials and Methods

Cell preparation and chemicals

D. discoideum Ax2, HM1038 (IP_3-receptor null mutant), the parental cell line Robert Kay's lab Ax2 (RK-Ax2), LW6 (Gβ-null mutant), the parental cell line DH1 and LW20 (Gβ-null mutant rescued with a Gβ-expressing plasmid) cells were grown at 21°C in axenic medium (Watts and Ashworth, 1970) in suspension on shakers rotating at 180 rpm(Ax2, RK-Ax2, HM1038) or in Petri dishes (DH1, LW6, LW20). The composition of the axenic medium is: 14.3 g l^{-1} Oxoid L34 peptone, 7.5 g l^{-1} Oxoid L21 Yeast Extract, 50 mM maltose, 5.33 mM Na_2HPO_4, 3.53 mM KH_2PO_4 and 0.34 mM dihydrostreptomycine. RK-Ax2 and HM1038 were obtained from the *Dictyostelium* Stock Center (http://www.dictybase.org/). Vegetative cells were harvested during exponential growth phase at a density of 2-4×10^6 cells ml^{-1}, pelleted by centrifugation (1000 ***g***, 4°C, 4 minutes), washed twice in Sörensen phosphate buffer (SB: 2 mM Na_2HPO_4, 14.5 mM KH_2PO_4, pH 6.2) or MES-Na buffer (20 mM morpholino ethane sulfonic acid, adjusted to pH 6.2 with NaOH) and used immediately. Glass plates or coverslips were cleaned with a ionic detergent and etched for 5 minutes with 14.5 M NaOH as previously described (Décavé et al., 2002). New glass plates or coverslips were used for each experiment.

Cell adhesion measurements

Cell adhesion to glass plates was measured in SB at different $CaCl_2$ concentrations in the presence of the cytoskeleton depolymerizing agent *N*-(3-chlorophenyl)isopropyl carbamate (CIPC) at a 2 μg ml^{-1} final concentration from a 10 mg ml^{-1} stock in DMSO, with a radial flow detachment assay (Décavé et al., 2002). Flow was applied during 15 minutes to complete the detachment kinetics. Results are given as critical shear stresses $\sigma_{50\%}$ (in Pa) that detach 50% of the cells.

Titration of extracellular calcium concentration

Calcium Green 2 (CG2, Molecular Probes, Interchim France) was added at a 1 μM final concentration to the solution, whose calcium concentration had to be determined. Known amounts of calibrated calcium or EGTA solutions were then added and the CG2 fluorescence was measured, subtracting the autofluorescence background. The data were fitted with the following equation:

$$\frac{F - F_{EGTA}}{F_{Ca} - F} = \frac{[Ca^{2+}]}{K_d}. \quad (1)$$

where F_{Ca} and F_{EGTA} are the maximum and minimum fluorescence levels (obtained at 1 mM $CaCl_2$ or EGTA, respectively), K_d the known CG2 dissociation constant (0.55 mM) and F the fluorescence level at the [Ca^{2+}] total calcium concentration (Rooney et al., 1994). The total calcium concentration is the sum of the unknown and the added calcium concentrations.

Cell motility experimental setup

Motility assays were conducted in a transparent lateral flow chamber using glass plates as previously described (Décavé et al., 2003). To visualize cell morphological changes during motility at a higher magnification, a new lateral flow chamber was built, designed on a similar overall basis, but using 25×60 mm^2 coverslips (Erie). In both cases, shear stress was calculated from geometrical and hydrodynamical parameters as:

$$\sigma = \frac{6D\eta}{le^2}, \quad (2)$$

where D is the flow rate, η the dynamic viscosity of the fluid, e the thickness of the flow chamber and l the width of the chamber.

Cell motility recording at low and high resolutions

To record shear-flow-induced motility at low resolution, cells were introduced into a glass plate flow chamber filled with SB or MES-Na buffer and allowed to adhere to the glass surface for 2 minutes. Unbound cells were removed by flowing buffer at a very low shear stress (0.1 Pa) from an upper tank. When needed, the fluid bathing the cells was replaced by flowing another solution for 3 minutes at low shear stress. Cell motility was triggered by the application of a constant larger shear stress and images were recorded every 15 seconds or 30 seconds during 10-15 minutes, depending on the expected cell speed. When indicated, calcium concentration was changed during the assay by exchanging the solutions flowing from different upper tanks using valves. Cells were observed at a 2.5× magnification under dark field illumination with a Zeiss EM405 inverted microscope. Images were taken by a SP-Eye cooled CCD video camera (Photonic Science, UK) controlled by the Image Pro Plus software (Media Cybernetics).

For high-resolution imaging using phase contrast, fluorescence or reflection interference contrast microscopy (RICM), cells were observed with a 60× oil objective on an inverted microscope (Olympus IX-71) under phase or episcopic illumination. Calcium Green 2 fluorescence was selected with a BGW cube (Olympus) and supplementary BG18 and BG28 excitation and emission filters (Melles Griot). Reflection Interference Contrast was obtained by selecting the 546 nm peak of the episcopic mercury lamp by a combination of interference and blue-green filters and illumination through an episcopic polarization cube. For all microscopic techniques, light intensity was reduced with neutral density filters, since high illumination intensities block cell movement.

To record phase contrast, CG2 fluorescence or RICM images during shear-flow-induced motility at high resolution, cells were introduced into a coverslip flow chamber in SB as described above. Typically, two kinds of experiments were performed. The first one consisted of applying shear stress to cells adapted to a given calcium concentration. The calcium concentration was raised to the indicated value at low shear stress, image recording was started (1 image per second) and a larger shear stress was applied 20 seconds later during 3 minutes. The second one consisted of varying the external calcium concentration around cells already submitted to shear-flow. A large shear stress was applied in SB, image recording was started (1 image per second) and the calcium concentration was raised during the experiment by flowing a 1 mM solution in SB from another upper tank. With valves located near the flow chamber, the calcium concentration was raised

in less than 10 seconds. It is important to note that the fluid level in the different tanks was precisely adjusted to avoid any pressure changes, since bending of the coverslip slightly changed cell position relative to the objective. In addition, focusing was adjusted during the run by visual inspection. Images were taken by an intensified cooled CCD video camera (Photonic Science, UK) mounted on an Olympus IX-71 inverted microscope, controlled by the Image Pro Plus software. Since exposure to even moderate light levels is harmful to cells, samples were renewed after 45 minutes.

Intracellular calcium visualization

To visualize intracellular calcium concentration changes, *Dictyostelium* cells were resuspended in SB containing 100 μM CG2 at 5×10^7 cells ml^{-1} in a 60 μl total volume and electroporated in a 2 mm wide cuvette at 4°C (electrical settings: 3 μF, 750 V, time constant: 2 milliseconds, Biorad electropulse apparatus). Cells were recovered with 1 ml SB supplemented with 5 mM $MgCl_2$ and 0.1 mM $CaCl_2$, pelleted by centrifugation (1000 ***g***, 4°C, 3 minutes), resuspended in 10 ml HL5 medium and incubated on a rotary shaker for 10 minutes at 21°C, after which they were introduced in a coverslip flow chamber as described above.

Quantitative analysis of cell motility

Individual cell tracks were reconstituted from low-resolution movies as described previously (Décavé et al., 2003). Cells that came into contact with other cells or that detached during the recording were excluded from the following analysis. For a given cell, the instant velocity is given by:

$$v_i(t_i) = \frac{\vec{c}_{i+1} - \vec{c}_{i-1}}{t_{i+1} - t_{i-1}}, \quad (3)$$

where $\vec{c}_i$ is the cell centroid position at time t_i. Speed and directionality are defined as the modulus of cell velocity and the cosine of the angle θ_i between the cell velocity and the direction of the flow, respectively, averaged over 30-40 cells:

$$\text{speed} = \langle \|\vec{v}_i\| \rangle , \quad (4)$$

$$\text{directionality} = \langle \cos\theta_i \rangle . \quad (5)$$

Dynamics of cell substrate contact areas

After recording RICM images, a background image obtained in the absence of cells was subtracted and the resulting images were segmented, using the Image Pro Plus software (IPP, MediaCybernetics). This generates a black and white movie showing the contact area evolution with time, where the cell-substrate contact areas appear white (pixel value 255) over a dark background (pixel value 0). The cell speed is defined as the mean velocity modulus of the center of mass of the contact area. Gain and loss zones are defined as the areas where the pixel value increases from 0 to 255, or decreases from 255 to 0, respectively, between two frames. The steady zone is the cell area where the pixel value stays constant. Mathematically, these areas are obtained by computing at each pixel the following function:

$$F_i = \frac{p_i - p_{i-3}}{6} + 127 + \frac{p_i}{255}, \quad (6)$$

where p_i is the pixel value at time t_i. The gained, lost or steady areas correspond to F_i=170, 86 or 128, respectively, and the background to 127. The running average over three frames (from t_i to t_{i-3}) eliminates the pixel noise associated to the numerical definition of the contact area edges. The gain and loss growth rates are defined as the cell area gained or lost by unit time.

$$\left(\frac{dA}{dt}\right)_{gain} = \frac{\text{gained area}}{t_i - t_{i-3}}, \quad \left(\frac{dA}{dt}\right)_{loss} = \frac{\text{lost area}}{t_i - t_{i-3}}. \quad (7)$$

A Visual Basic IPP macro was written to perform these operations, generate a colored movie and send the values of the gain and loss growth rates along time to an Excel datasheet. This program is available upon request.

The gained and lost area growth rates are then plotted as a function of time and smoothed with a Savitzky and Golay algorithm. A 7- or 11-point algorithm is used for gain and loss growth rates, respectively. The position and values of the peaks and valleys are extracted. Peaks whose height is less than 0.2 $\mu m^2\ s^{-1}$ over that of a neighbor valley are rejected because the existence of the peak is not significant compared with the pixel noise. Finally, for each recording, peak height and frequency are computed. The peak height is defined as the average value of all peaks. The peak frequency is defined as the inverse of the average time separating two successive peaks.

Results

External calcium entry is required for efficient shear-flow-induced cell motility

Application of shear-flow triggers a cellular response in *D. discoideum* cells resulting in a net cell movement in the direction of the flow (Décavé et al., 2003). Analysis of the movement showed that both the modulus and orientation of cell velocity was affected by shear stress. Furthermore, PI3K activity was required for cells to move in the direction of the flow, but not for cells to move quicker in response to the flow. Speed and directionality of cell movement are therefore independently regulated. More recently, we noticed experimental variations in cell velocities whose origin was tracked down to the Sörensen phosphate buffer solution used for the experiments. In this medium, calcium concentration is not controlled and depends on water purity (3-6 μM for distilled water). We found that external calcium concentration is a key parameter to stimulate shear-flow-induced cell motility.

Fig. 1 shows cell responses to shear-flow at different external calcium concentrations. Raising the calcium concentration from <10 μM up to 1 mM moderately increases cell speed in the absence of the flow, but stimulates it fivefold in the presence of a 2.4 Pa shear stress (Fig. 1A, see also supplementary material, Movies 1 and 2) also marginally enhanced under these conditions (Fig. 1B). Conversely, lowering calcium concentration to about 0.4 μM by chelation with 100 μM EGTA instantaneously decreases cell speed (Fig. 1C). This effect is reversible since cell movement resumes when the external calcium concentration is increased again (Fig. 1C). In the continuous presence of 100 μM EGTA, cell motility spontaneously recovers after 5 minutes (data not shown), suggesting that cells adapt to low external calcium concentrations. In addition to its effect on cell motility, Ca^{2+} chelation also induces significant cell detachment from the substrate, which will be quantified below. Addition of 100 μM Gd^{3+}, a known inhibitor of plasma membrane Ca^{2+}-channels, reversibly and competitively stops cell movement (Fig. 1D). No spontaneous recovery is observed in this case. The possible role of magnesium, sodium and potassium ions was also addressed using alternative buffer formulation (MES-Na or MES-K buffers supplemented with $MgCl_2$ or $CaCl_2$, see

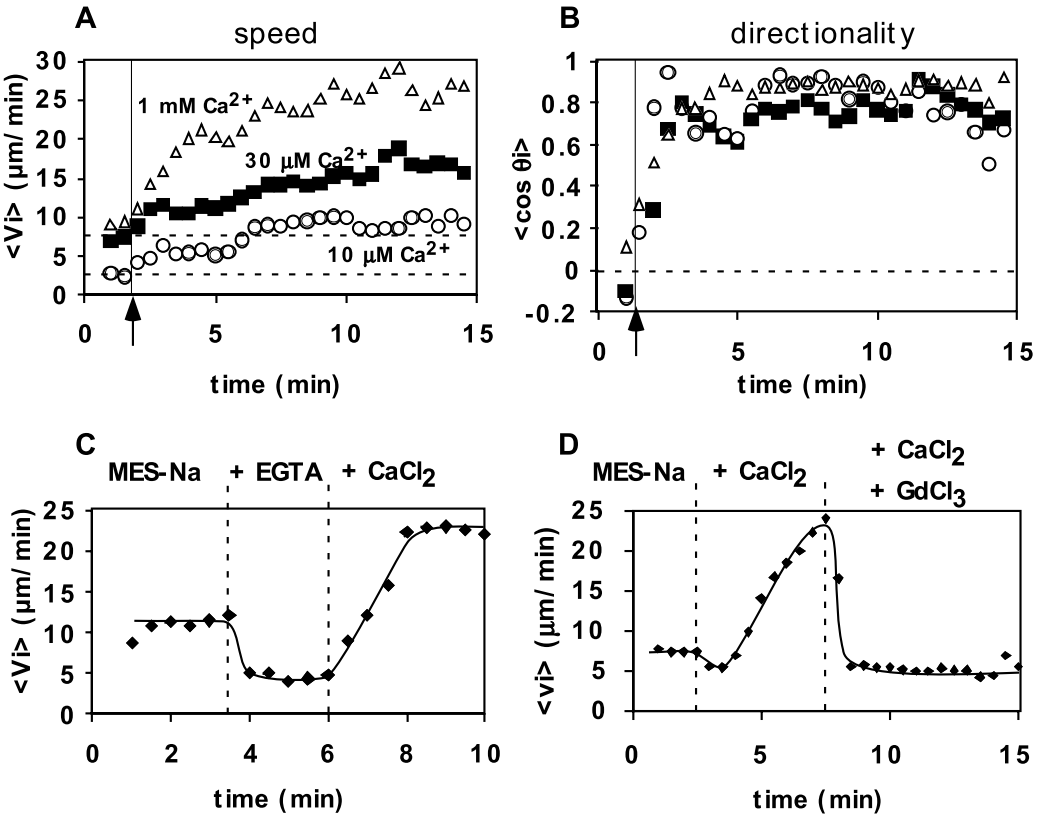

Fig. 1. Calcium entry is required for shear-flow-induced cell motility. (A,B) Ax2 cells were allowed to adhere to glass at a low (5-10 µM) calcium concentration, then the calcium concentration was raised to the indicated value by changing the bathing solution at low shear stress. The flow was then stopped and video recording started (t=0 minutes). After 2 minutes, a constant shear flow (2.4 Pa) was applied (arrow). The instant cell speed (A) and directionality (B) are plotted as a function of time. ○, ■ and △: 10 µM, 30 µM and 1 mM $CaCl_2$, respectively, added to MES-Na buffer. Standard deviations in (A) and (B) are 3 µm minute^{-1} and 0.1, respectively (data not shown). (C,D) Cells were allowed to adhere to glass at a low (5 µM) calcium concentration (MES-Na buffer), then a constant shear flow (2.4 Pa) was applied and video recording started (t=0 minutes). (C) At the indicated times, the flowing solution was exchanged, first for MES-Na buffer supplemented with 100 µM EGTA, then for MES-Na buffer supplemented with 1 mM $CaCl_2$. (D) The same procedure was applied, except that MES-Na buffer was first supplemented with 1 mM $CaCl_2$, then with 1 mM $CaCl_2$ + 100 µM $GdCl_3$. The average instant cell speed $\langle v_i \rangle$ is plotted as a function of time.

supplementary material, Table S1). None of the tested ions but calcium was found to be specifically required for cell motility. Finally, extracellular pH was varied from 5 to 7 using MES and phosphate buffers. No change in cell speed nor directionality was observed between pH 6 and 7, ruling out a significant role of transmembrane pH gradients in cell motility (supplementary material, Table S1). Altogether, these results show that calcium channels are active at the plasma membrane and that calcium entry stimulates cell motility for cells submitted to shear stress.

Using cell speed as a measure of cell response to shear stress and raising or lowering the external Ca^{2+} concentration in the bathing fluid, we can plot the characteristic dose-response curve (Fig. 2A). To avoid any precipitation between calcium and phosphate in SB, these experiments were conducted in the presence of 20 mM MES-Na buffer (pH 6.2). Data are fitted with a single hyperbolic curve, suggesting that Ca^{2+} interacts mainly with a single class of targets ($K_{50\%}$=22 µM). The direct effect of calcium on passive cell adhesion to glass was also investigated, measuring $\sigma_{50\%}$ as a function of Ca^{2+} concentration in a radial flow chamber. This parameter is the shear stress at which half of the cells detach and is directly related to the interaction energy between adhesion protein complexes and the substrate (Décavé et al., 2002). Radial flow detachment assays were conducted in the presence of CIPC, to uncouple passive adhesion from cytoskeleton dynamics (Décavé et al., 2002; Décavé et al., 2003). Fig. 2B shows that *D. discoideum* binding to glass in the presence of SB or MES-Na buffer is sensitive to calcium concentration, but the 'apparent affinity' for $\sigma_{50\%}$ is ten times smaller than for cell speed ($K_{50\%}$=2.5 µM). The calcium target affecting cell adhesion is therefore distinct from that affecting cell motility.

Cell motility was then examined as a function of applied shear stress, at either low (5 µM) or high (1 mM) calcium concentration. We previously reported that above 1 Pa, shear stress invariably triggers an increase in cell speed and directional motility with the flow (Décavé et al., 2003). Enhancement of cell speed with more calcium and longer recording periods allow observing additional cell behaviors at intermediate shear stresses. Typical results are exemplified on Fig. 3A,B, where cell speed (panel A) and directionality (panel B) are shown as a function of time. Shear stresses under 0.1 Pa trigger a hardly detectable motile response. Application of intermediate shear stresses (between 0.1 and 0.6 Pa) gives rise to a complex cell response. On short time (<2 minutes), cell speed increases and cell movement is oriented along the flow. On longer time (>2 minutes), cell speed decreases slightly and cells tend to move against the flow (see also supplementary material, Movie 3). Higher shear stresses (>0.6 Pa) only trigger cell movement in the direction of the flow, but a decrease in cell speed and directionality is noticeable after 2 minutes. Cell motile response, therefore, can be divided into an immediate and adapted phase. During the immediate phase, cells move in the direction of the flow, while in the adapted phase, they move against or along the flow depending on the shear stress value. These results are quantitatively summarized in Fig. 3C,D, where cell speed and directionality in the adapted phase are

Journal of Cell Science

Journal of Cell Science

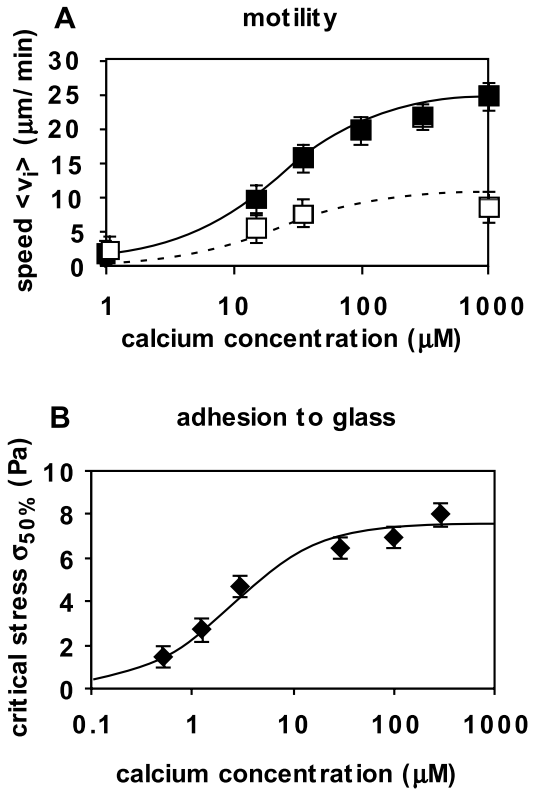

Fig. 2. Calcium requirements for cell motility and cell adhesion to glass. (A) The average cell speed is plotted as a function of the free calcium concentration in the bathing fluid, for cells submitted to shear stress (2.4 Pa, ■) or not (□). In the first case, the average cell speed is determined in the steady-state portion of the motility response (from 8 to 15 minutes after onset of the flow, see Fig. 1), except when EGTA is added (1 µM), where it is determined 30 seconds to 3 minutes after EGTA addition (see Fig. 1C). In the second case, the average cell speed is determined from the entire recording. The solid and the dashed lines correspond to a fit with an apparent calcium affinity of 22 µM and a maximum speed of 25 and 10 µm minute^{-1}, respectively. Standard deviation is 2 µm minute^{-1} (data not shown). (B) The critical shear stress for cell detachment is plotted as a function of the calcium concentration in the flowing fluid. Ax2 cell adhesion was probed with the radial flow detachment assay. The solid line corresponds to a fit with an apparent calcium affinity of 2.5 µM and a maximum detachment shear stress of 7.5 Pa. Error bars, 0.5 Pa (data not shown). Free calcium concentrations above or below 5 µM were obtained by adding $CaCl_2$ or EGTA, respectively to MES-Na buffer (A) or SB (B).

plotted as a function of shear stress under low or high calcium concentrations. Again it is clear that calcium does not affect cell directional orientations but makes cells faster in response to shear flow. Half-maximum speed is reached at 0.5 Pa and 3.5 Pa at 1 mM and 5 µM calcium concentrations, respectively.

An increase of cell speed is also observed when calcium concentration is raised under constant shear stress (Fig. 4A,B). As calcium enters the flow chamber, cell speed first slightly decreases during about 1 minute, then it increases for 3-5 minutes then it returns to its low calcium concentration level in about 15 minutes. Again, almost no change is observed on cell directionality. This transient acceleration is concomitant with a striking change in cell morphology (Fig. 4C,D, see also supplementary material, Movie 4). *Dictyostelium* cells examined 2 minutes after calcium rise are elongated, with one or a few large round protrusions at the front edge (Fig. 4C, white arrowheads) and a triangular retraction zone at the rear edge, very much looking as chemotaxing neutrophils (Xu et al., 2003). Furthermore, cell movement appears very smooth, with almost no side protrusions. In many occurrences, the front edge of the cell rhythmically moves, with a 9-12 seconds time period (see supplementary material, Movie 4, bottom cell and top right cell). Cells observed before the calcium rise or 15 minutes later present several smaller protrusions extending from the front edge (Fig. 4D, black arrowheads), without any structure clearly associated with the retracting parts. These results show that plasma membrane calcium channels are open in motile cells, and that their number or activity are regulated in response to shear stress and to external calcium concentration changes.

Cell edge dynamic is stimulated by the presence of external calcium

To understand the origin of the increased cell motility with calcium, cell-substrate contact areas were imaged by RICM during shear-flow-induced motility. Because of the time needed to focus on single cells, these experiments were done several minutes after exposing the cells to shear flow. At each calcium concentration, series of movies were obtained, where the dark areas correspond to zones of close proximity between the cell and the substrate (see supplementary material, Movies 5-7).

The previous analysis of the movies consisted of determining the position of the front and rear edges of the cell along the direction of the movement (Décavé et al., 2003). The front edge moves through fast extensions (bursts), separated by immobility phases whereas the rear edge moves more smoothly. Such analysis conducted on recorded movies shows that burst length increases with the external calcium concentration (data not shown). However, at calcium concentrations higher than 100 µM, many cell extensions correspond to the formation of new contact zones rather than to the lateral extension of existing ones. A new image analysis procedure was therefore designed, so that gained and lost contact areas between successive image frames are detected (see Materials and Methods). A color model of the cell-substrate contact areas is generated, where the gained areas are blue, the lost ones red and the steady areas green (see supplementary material, Movies 8-10). The areas gained and lost between successive frames, divided by the time interval, give the gained and lost area growth rates, respectively. They are plotted on Fig. 5A as a function of time, for individual cells at different calcium concentrations. At 5 µM calcium, the gained area growth rate is irregular, with large peaks separated by periods of reduced activity. Large peaks correspond to bursts detected in the previous analysis. As for the lost area growth rate, almost no organization appears over a steady 1 µm^2 s^{-1} loss rate. At larger calcium concentrations, the gain and loss growth rates appear much more regular, with peaks of high activity repeating at 9-11 seconds time intervals. Representative examples are shown, that were recorded at 100 and 300 µM calcium concentrations (Fig. 5A). Periodic occurrence of protrusions and retractions is especially noticeable on Movie 10 (see supplementary material) (Fig. 5A

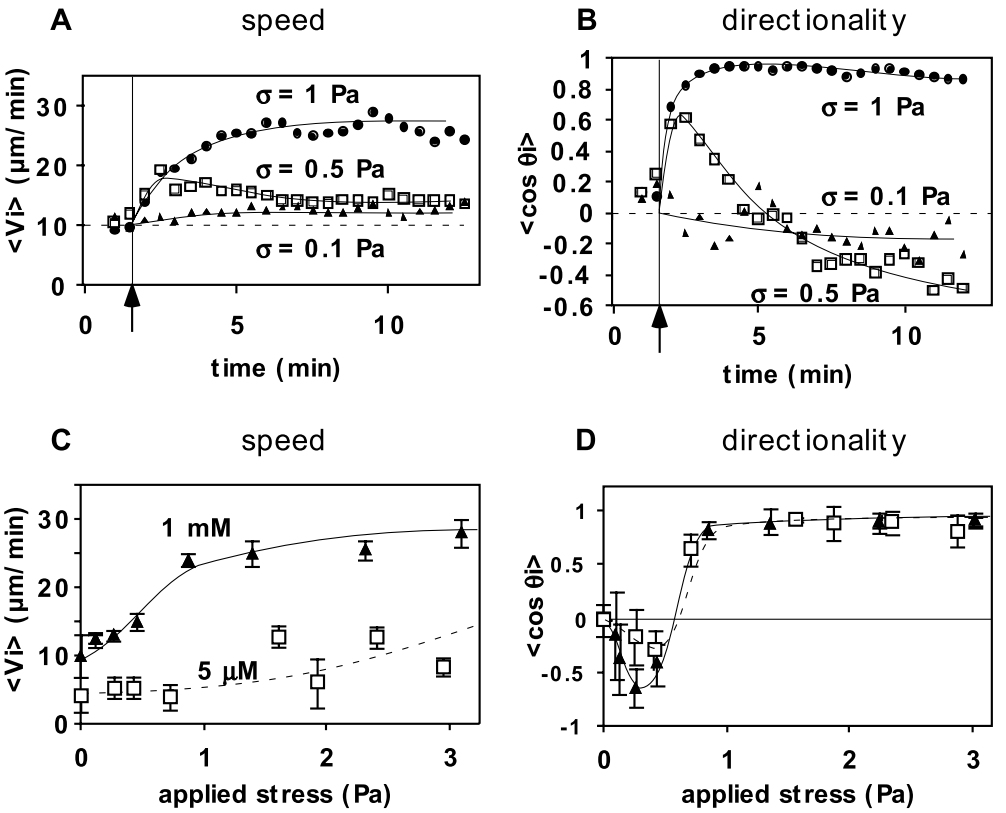

Fig. 3. Force sensitivity is modulated by the external calcium concentration. (A,B) Ax2 cells were allowed to adhere to glass at a low (5-10 µM) calcium concentration in MES-Na buffer, after which the calcium concentration was raised to 1 mM at low shear stress. The flow was then stopped and video recording started (t=0 minutes). After 2 minutes, a constant shear stress was applied (arrow): ▲, σ=0.1 Pa; □, σ=0.5 Pa; circles, σ=1 Pa. The instant cell velocity modulus (A) and directionality (B) are plotted as a function of time. (C,D) Average cell speed (C) and directionality (D) are plotted as a function of the applied shear stress at a 1 mM (▲) or 5 µM (□) calcium concentration. The average cell speed and directionality are determined from the steady-state portion of the motility response to shear stress (from 7 to 15 minutes in Fig. 3A,B). Data are collected from several independent experiments performed in Sörensen or MES-Na buffer.

300 µM calcium: 90-150 seconds left panel, 30-90 seconds right panel). Periodic protrusive activity is also noticeable at low calcium concentration on the graph. A similar analysis was performed on ten cell recordings and, for each of them, the average height of the peaks and the average time between successive peaks were calculated. These parameters are plotted on Fig. 5B,C as a function of the average cell speed during the recording. A good correlation is found between the gain and loss peak height and cell speed, whereas peak frequency is constant, whatever the calcium concentration. The frequency of protrusions is slightly larger (0.11±0.01 Hz) than that of retractions (0.08±0.01 Hz)[†].

The cell speed increase due to external calcium therefore results from a stimulation of cell spreading and retraction activities. This stimulation acts on the protrusion and retraction area growth rates but not on the frequency of these events.

As an attempt to visualize possible internal calcium concentration variations during cell movement, cells were loaded with the calcium indicator CG2. Spreading of these CG2-loaded cells to glass absolutely required addition of at least 100 µM calcium in the external medium and full reconstitution of movement was obtained only after allowing cells to recover in growth medium (see Materials and Methods). The calcium requirement for spreading again proves the existence of a calcium influx coupled to the deformation of cell cortex. The same effect was observed with other calcium indicators at a similar concentration. Within the cells, CG2 fluorescence accumulated in vesicles of different sizes in addition to a uniform, probably cytosolic distribution. Neither gross variation of the uniform fluorescent background nor a clear intracellular gradient was observed in cell undergoing fast shear-flow-induced motility. Periodic protrusive and retractile activities associated to cell movement therefore do not correspond to large intracellular calcium fluctuations. Interestingly, in most cells, a fluorescent zone was observed at the cell rear, whose intensity rhythmically fluctuated (see supplementary material, Movie 11). With a period of about a minute, fluorescence steadily increased then suddenly decreased. Alternating phase contrast and fluorescence illuminations showed that this oscillation originates from the contractile vacuole activity, which presumably pumps CG2 out of the cell through a calcium-rich compartment as discussed previously (Rooney et al., 1994).

Heterotrimeric G proteins are involved in calcium stimulation of shear-flow-induced cell motility

To test for the involvement of heterotrimeric G proteins in shear-flow-induced *Dictyostelium* cell motility, a mutant cell line was used, LW6, where the single gene coding for the β-subunit of this protein family was removed by homologous recombination (Lilly et al., 1993; Wu et al., 1995). At 5 µM calcium concentration, Gβ-null cells exhibit directional motility in response to shear stress, comparable with that of the parental DH1 cell line. Similarly, lowering calcium concentration with EGTA blocks cell motility and induces its detachment (data not shown). Increasing calcium concentration

[†]There is not any contradiction between the conservation of the average cell-substrate contact area during the movement and the fact that protrusion and retraction growth rates have the same amplitude and different frequencies. Consider an ideal situation where the gained or lost area growth rate dA/dt is modeled by a sinusoidal function: $dA/dt=A_0+A_1\cos(\omega t)$. On average, $\langle dA/dt\rangle=A_0$, whatever the frequency $2\pi/\omega$. The maximum amplitude of the peaks is A_0+A_1. Our results show that A_0 and A_1 are similar for protrusions and retractions and ω is different.

Journal of Cell Science

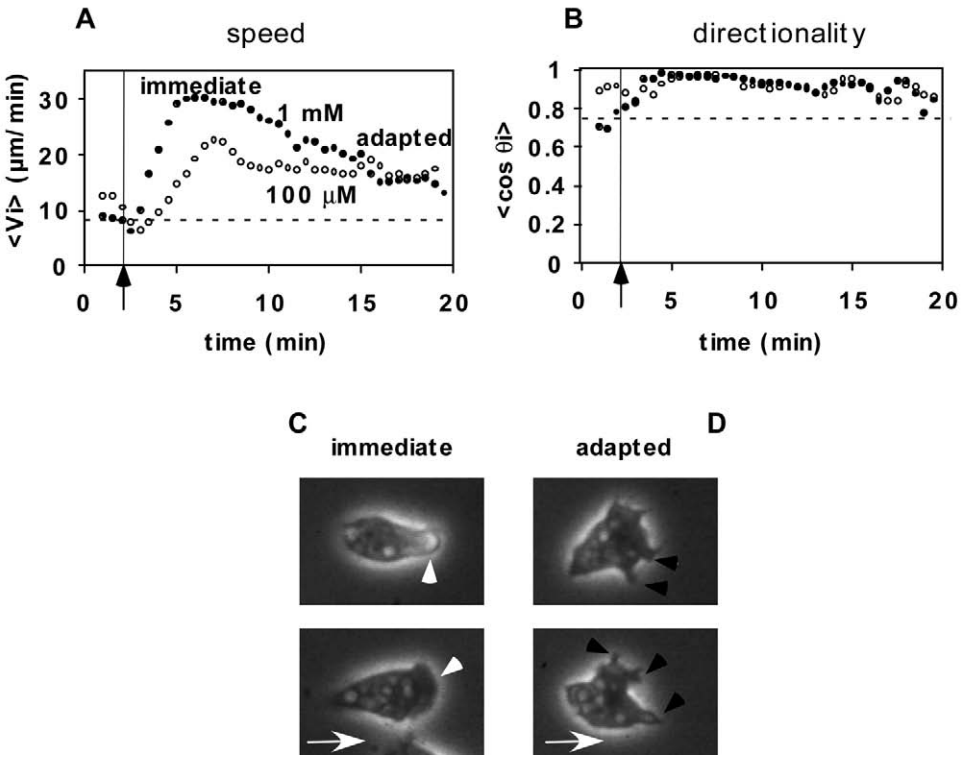

Fig. 4. Cell speed increases and cell morphology changes upon a rise of extracellular calcium concentration under applied stress. (A,B) Ax2 cells were allowed to adhere to glass at a low (5-10 µM) calcium concentration in MES-Na buffer, then a constant shear stress (2.4 Pa) was applied and video recording started (t=0 minutes). After 2 minutes, the calcium concentration was raised to 1 mM (●) or 100 µM (open circles) at the same shear stress. The instant cell velocity modulus (A) and directionality (B) are plotted as a function of time. (C,D) High-resolution imaging of cells undergoing shear-flow-induced motility (σ=2.4 Pa) in the presence of 1 mM $CaCl_2$. Cells were imaged during either the immediate (C) or the adapted (D) phases, defined as on Fig. 4A. In C are shown examples of the large protrusions frequently observed when calcium is raised under shear stress (white arrowheads). In D are shown small protrusions observed either at low calcium concentrations or when cells are adapted to the extracellular calcium concentrations (black arrowheads).

however does not speed up cell movement. This is quantitatively shown in Fig. 6A, where cell speed is plotted as a function of the external calcium concentration. As shown before, results are fitted with a single class of Ca^{2+} sites whose affinity is not measurable for Gβ-null cells ($G\beta^{\Delta}$) cells ($K_{50\%}$>1000 µM). Expression of a Gβ gene in Gβ-null cells partially restores Ca^{2+} sensitivity to shear-flow-induced motility ($K_{50\%}$=150 µM). The speed of Gβ-null cells is also much less sensitive to external shear stress than the rescued ones in the presence of millimolar calcium (Fig. 6C). However, directional sensing is marginally affected by the lack of the heterotrimeric G protein β-subunit, since clear orientation in the direction of the flow occurs at shear stresses higher than 1.7 Pa for Gβ-null cells and 1.5 Pa for the rescued ones (Fig. 6D). Furthermore, when calcium concentration is raised from the micromolar to millimolar levels under constant shear flow, no change in cell speed is recorded for Gβ-null cells, whereas the rescued cells accelerate, albeit more slowly than Ax2 wild-type cells (Fig. 6B). These results suggest that calcium channels are closed in Gβ-null cells under shear flow.

Cell-substrate contact area was also imaged for Gβ-null cells under shear flow at different calcium concentrations and its dynamics was compared with that of the rescued cells. Protrusion and retraction dynamics are analyzed as explained above and shown in Fig. 7. Whatever the calcium concentration, the growth rate activity of Gβ-null cells is low and comparable with that of wild-type cells at 5 µM calcium (Fig. 7A and see supplementary material, Movie 12). By contrast, the gained or lost area growth rates of Gβ-rescued cells exhibit larger periodic activity at calcium concentrations higher than 100 µM. This is quantitatively shown on Fig. 7B,C. Peak heights of protrusion and retraction growth rates do not increase with cell speed for Gβ-null cells, whereas they increase three times for rescued cells. For both cell lines, protrusion and retraction peak frequencies are almost independent of the calcium concentration and comparable with that of Ax2 cells (0.13±0.01 Hz and 0.09±0.02 Hz, respectively). A reduction of the gain and loss growth rates therefore accounts for the lower motility of Gβ-null cells. Plasmid expression of Gβ restores calcium sensitivity to both cell speed and protrusive and retractile activities.

A *Dictyostelium* IP_3-receptor like protein amplifies calcium stimulation of shear-flow-induced cell motility

In higher eukaryotic cells, heterotrimeric G proteins activate phospholipase C β-isoform, which cleaves membrane-bound PIP_2 into diacylglycerol (DAG) and inositol 1,4,5-trisphosphate (IP_3). In turn, soluble IP_3 triggers intracellular calcium release from the endoplasmic reticulum by binding to a specific IP_3-receptor. In *Dictyostelium*, a single PLC isoform is known, which belongs to the δ-isoform family and is activated by calcium (Cubitt and Firtel, 1992; Drayer et al., 1994). In addition, an IP_3-receptor-like gene was found (*iplA*), whose disruption produces null cells in which Ca^{2+} entry in response to chemoattractants is greatly reduced (Traynor et al., 2000). Nevertheless IP_3-receptor null cells are still able to chemotax toward cAMP, and cAMP or cGMP productions in response to a cAMP pulse are normal.

We measured shear-flow-induced motility of IP_3-receptor null cells and the parental RK-Ax2 cells. Cells from both strains move in the direction of the flow and are sensitive to external calcium concentrations but IP_3-receptor null cells requires more calcium to reach the same speed than wild-type cells (Fig. 8A). The mobilization of internal Ca^{2+} stores is therefore a major contributor to cell speed under shear stress.

Journal of Cell Science

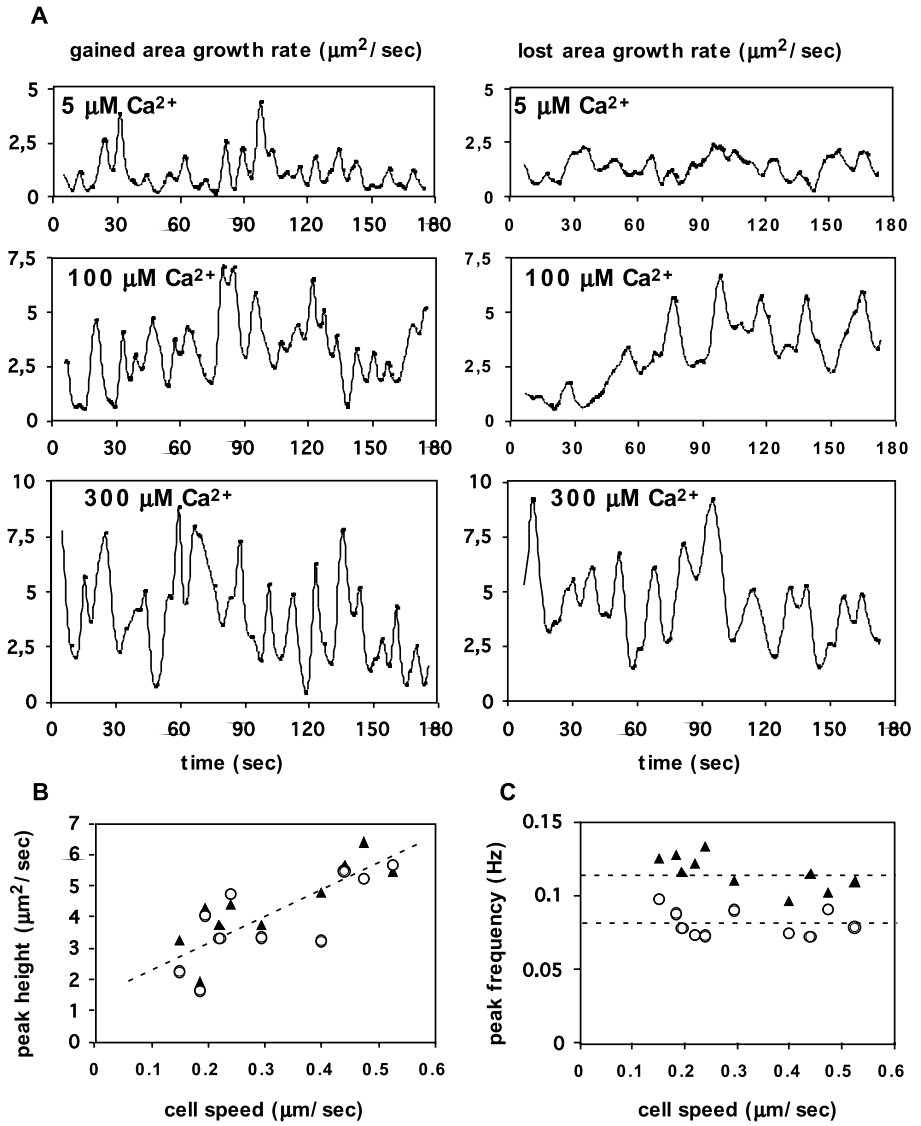

Fig. 5. Dynamics of cell-substrate contact areas during shear-flow-induced motility. Ax2 cells undergoing shear-flow-induced motility (σ=2.4 Pa) in the presence of the indicated calcium concentration were imaged at high resolution under RICM and morphology of cell-substrate contact areas was analyzed as described in Materials and Methods. (A) Growth rates of gained (left) and lost (right) contact areas are represented as a function of time, for individual cells recorded at the indicated calcium concentration. Average peak height and frequency are determined from such recordings. (B,C) Average peak height and frequency are plotted as a function of cell speed, for ten individual cells. ▲, protrusions; ○, retractions. In B, the dotted line is a linear least square fit of all data points (slope 7.9 μm; ordinate at origin 1.7 μm^2 $second^{-1}$). Standard deviations for protrusion and retraction peak heights are 1.9 and 1.3 μm^2 $second^{-1}$, respectively. In C, the dotted lines represent the mean values of the retraction and protrusion frequencies.

In addition, the directionality of the movement of the mutant cells is significantly lower at low calcium concentration (Fig. 8B). Furthermore, although IP_3-receptor null cells accelerate in response to an increase of the external calcium concentration, they do so much more slowly than the parental RK-Ax2 cells (Fig. 8C) and their movement is less directional (Fig. 8D). The dynamics of cell substrate contact area of IP_3-receptor null cells is similar to that of wild-type cells, although at a given calcium concentration, protrusion and retraction growth rates peak at smaller values (data not shown). The simplest interpretation is that calcium influx is much reduced in IP_3-receptor null cells, as reported for the cAMP or folate response of these cells (Traynor et al., 2000). Another possibility is that calcium influx has less effect inside IP_3-receptor null cells. The underlying mechanistic assumption is in the former case, that internal calcium release triggers external calcium entry (capacitive calcium uptake) or in the latter case, that external calcium entry triggers internal calcium release (calcium-induced calcium release).

In conclusion, the presence of heterotrimeric G proteins, the IP_3-receptor-like protein and an external calcium concentration above 30 μM are required for rapid actin cytoskeleton reorganization, resulting in efficient cell motility.

Discussion

This work provides evidence for the involvement of Ca^{2+} and heterotrimeric G protein signaling in adhering cells submitted to shear flow. More precisely, G protein activation is necessary for cells to modulate their speed in response to shear stress, through activation of plasma membrane calcium channels and IP_3-mediated internal calcium store release. Vegetative cells lacking G proteins indeed behave similarly to wild-type cells exposed to shear stress in the presence of low (e.g. 5 μM) calcium concentrations, although they possess the machinery to uptake calcium in response to folic acid (Nebl et al., 2002). Cells lacking the IP_3-receptor require higher external Ca^{2+} concentrations to reach the same speed as wild-type cells. However, neither G protein activation nor Ca^{2+} entry is necessary for directional sensing. On the contrary, PI3K activity is necessary for directional sensing, but not for the stimulation of speed by shear stress (Décavé et al., 2003). It follows that, for the mechanosensing response, heterotrimeric G proteins do not activate PI3K. This suggests that exposure to shear stress involves two signaling pathways in *Dictyostelium* cells, one which activates G proteins, is sensitive to calcium and controls cell speed, and another one which results in the production of a PIP_3 gradient and defines cell orientation (Fig. 9). Interestingly, PIP_2 appears to be at the crossroad between the direction and speed pathways, since it is the source of both PIP_3 and IP_3. In this respect, it is indicative that IP_3-receptor null cells exhibit both speed and orientation defects.

Different effects are observed, depending on the calcium concentration level. (1) At low concentration (<10 μM), calcium is necessary for *Dictyostelium* binding to glass. In addition, competition between cell-cell and cell-glass adhesion is observed in the flow chamber at high cell concentration (data not shown). This suggests that cell-cell contact and cell-glass adhesion share the same molecular receptor, which could be DdCAD-1 (also known as contact site B or gp24), a protein belonging to the large Ca^{2+}-dependent cadherin family (Chadwick et al., 1984; Knecht et al., 1987; Wong et al., 1996). Interestingly, DdCAD-1 interacts with catenin (Coates and Harwood, 2001; Grimson et al., 2000) and talin (Niewohner et al., 1997) homologs. The physiological significance of shear-flow-mediated motility could therefore be related to the formation and disruption of homotypic cell contacts. (2) At higher extracellular calcium concentration (between 10 μM and 100 μM), calcium enters the cell and speeds up both membrane spreading and retraction. Our results show that calcium influx through the plasma membrane occurs during cell motility. This is indicated by the effect of the competitive

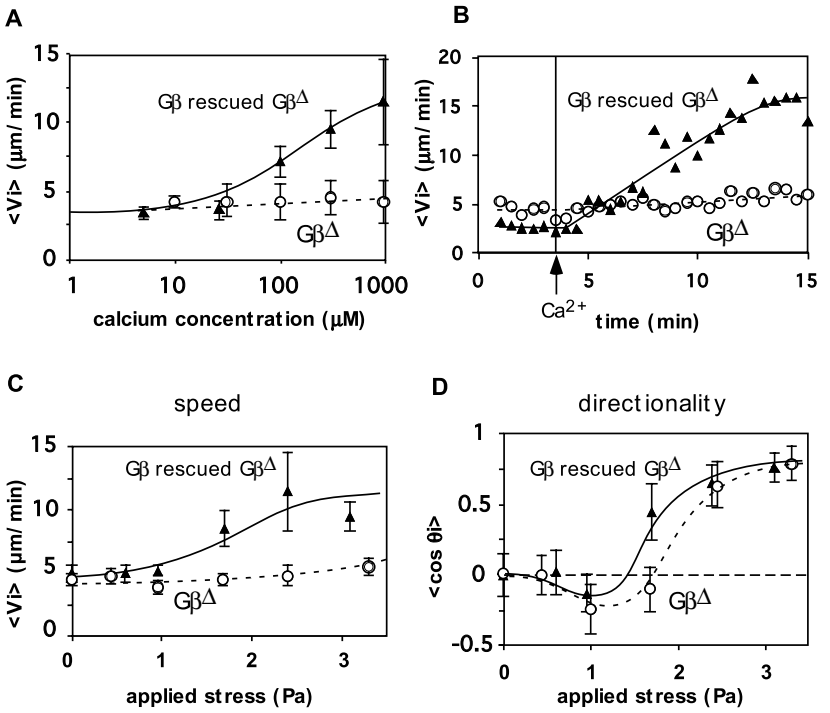

Fig. 6. Cells devoid of the β subunit of the heterotrimeric G protein family are insensitive to an increase of the external calcium concentration. (A) Average speed of LW6 Gβ-null cells (GβΔ, ○) or LW20 Gβ-rescued cells (Gβ-rescued GβΔ, ▲) is plotted as a function of the free calcium concentration in the flowing fluid (σ=2.4 Pa). The solid line corresponds to a fit with an apparent calcium affinity of 150 μM and a minimum and maximum speed of 3.5 and 13 μm $minute^{-1}$, respectively. (B) LW20 (Gβ-rescued GβΔ, ▲) and LW6 (GβΔ, ○) cells were allowed to adhere to glass at a low (5 μM) calcium concentration, then a constant shear stress (2.4 Pa) was applied and video recording started (t=0 minutes). After 2 minutes, the calcium concentration was raised to 1 mM at the same shear stress. Instant cell speed is plotted as a function of time. Note that at low calcium concentrations, LW6 cell speed is slightly, but significantly higher than that of LW20 cells. (C,D) Average cell speed (C) and directionality (D) are plotted as a function of the applied shear stress at a 1 mM calcium concentration either for LW20 (Gβ-rescued GβΔ, triangles) or LW6 (GβΔ, ○) cells. Average cell speed and directionality are determined from the steady-state portion of the motility response to shear stress.

Fig. 7. Protrusions and retractions are less active during shear-flow-induced cell motility in cells devoid of the beta subunit of the heterotrimeric G protein family. LW6 or LW20 cells undergoing shear-flow-induced motility (σ=2.4 Pa) in the presence of the indicated calcium concentration were imaged at high resolution under RICM and morphology of cell-substrate contact areas was analyzed as described in Materials and Methods. (A) Growth rates of gained (left) and lost (right) contact areas are represented as a function of time, for a single Gβ-null cell at a 1 mM calcium concentration. (B,C) Mean peak height and frequency are plotted as a function of individual cell speed. △, ▲ protrusions; ○, ● retractions. Filled symbols, Gβ-rescued cells (LW20); open symbols, Gβ-null cells (LW6). In B, the dotted line is a linear least square fit of the LW20 data points (slope 4.9 μm; ordinate at origin 0.7 μm^2 $second^{-1}$). Standard deviations for protrusion and retraction peak height are 0.9 and 0.7 μm^2 $second^{-1}$ for Gβ-null cells and 0.7 and 0.5 μm^2 $second^{-1}$ for Gβ-rescued cells, respectively. In C, the dotted lines represent the mean values of the retraction and protrusion frequencies.

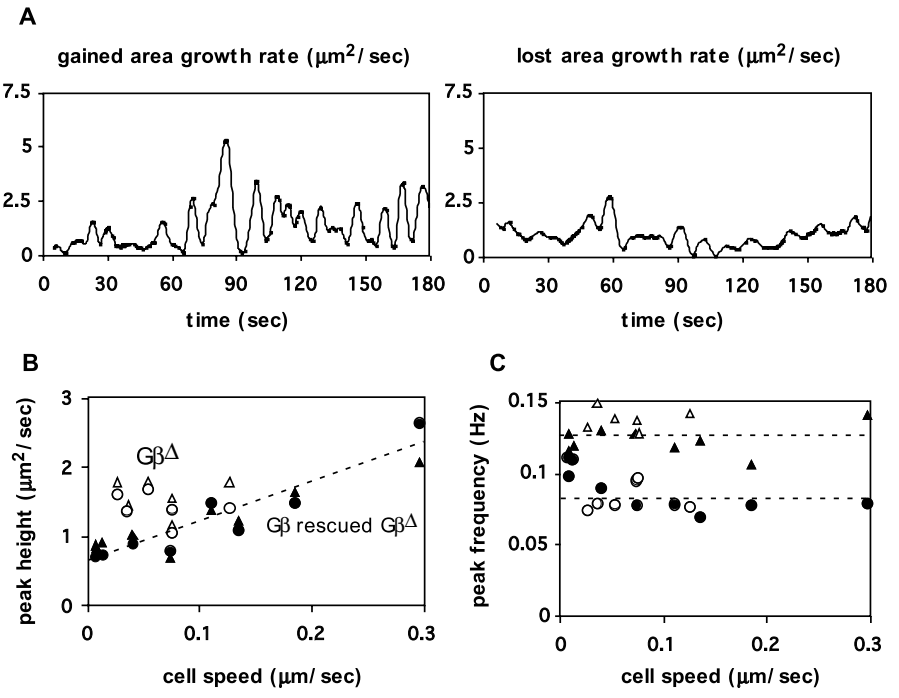

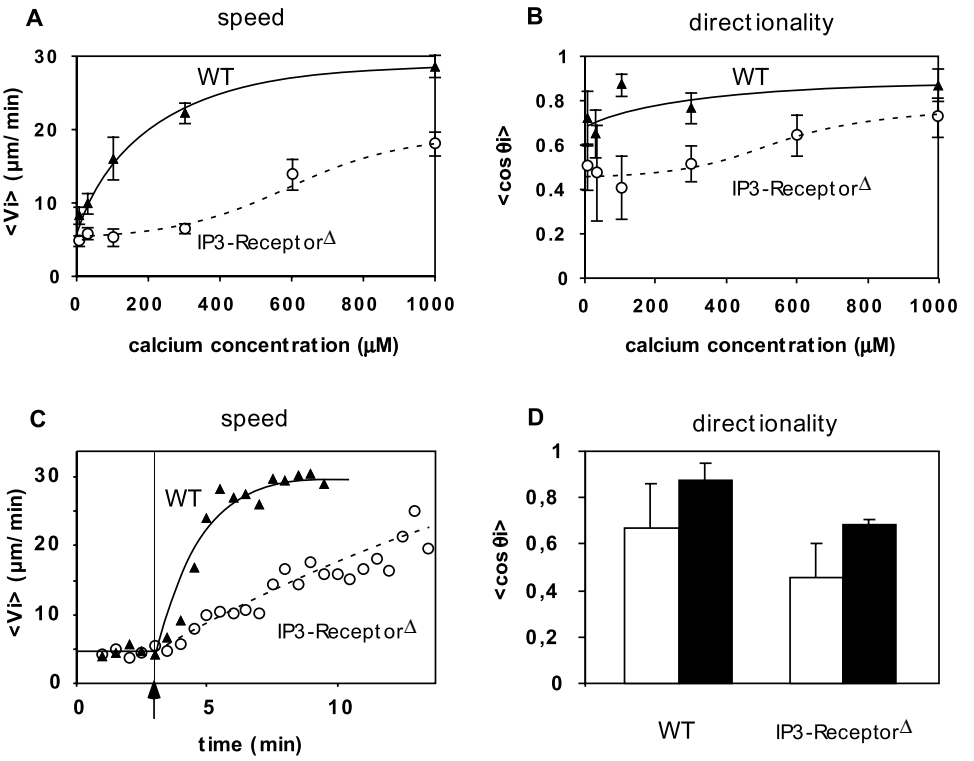

Fig. 8. Shear-flow-induced motility of IP_3-receptor null *Dictyostelium* cells. (A,B) Average speed (A) and directionality (B) of IP_3-receptor null cells (IP_3-Receptor$^{\Delta}$, circles) or parental RK-Ax2 cells (wild type, triangles) are plotted as a function of the free calcium concentration in the flowing fluid (σ=2.4 Pa). The solid line corresponds to a fit with an apparent calcium affinity of 120 µM and a minimum and maximum speed of 5 and 32 µm minute^{-1}, respectively. The dotted line is a guide for the eye. (C,D) IP_3-receptor null cells (IP3-Receptor$^{\Delta}$, ○) or parental Ax2-RK cells (wild type, ▲) were allowed to adhere to glass at a low (5 µM) calcium concentration, then a constant shear-flow (2.4 Pa) was applied and video recording started (t=0 minutes). After 3 minutes, the calcium concentration was raised to 1 mM under the same shear stress. (C) Cell speed is plotted as a function of time. The lines are hand-drawn. (D) Cell directionality is measured during the 1-3 minutes (white bars) and 8-12 minutes (black bars) portions of the recordings, corresponding to a 5 µM and 1 mM extracellular concentration, respectively.

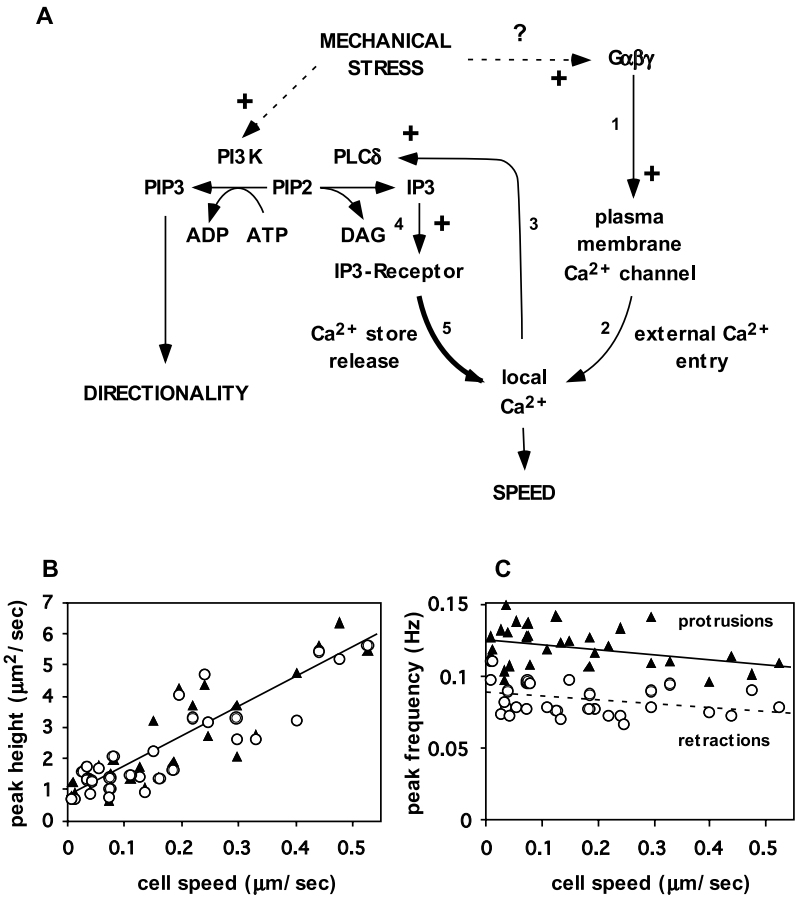

Fig. 9. (A) Model of *Dictyostelium* signaling pathways involved in shear stress-induced motility. Experimental evidence supporting a role for PI3K in the directionality response is presented elsewhere (Décavé et al., 2003). A link between mechanical stress and heterotrimeric G protein activation is shown in the present work since Gβ-invalidation reduces cell speed in response to shear stress (Fig. 6C). In both cases, molecular details are unknown. Heterotrimeric G protein mediated Ca^{2+} entry (arrows 1 and 2) is supported by the effect of Gd^{3+} ions (Fig. 1D) and Gβ-invalidation (Fig. 6B). Ca^{2+}-induced PLCδ activation (arrow 3) is shown in (Cubitt and Firtel, 1992). Direct biochemical evidence for IP_3-mediated calcium release (arrows 4 and 5) is given elsewhere (Schaloske et al., 2000). Our work suggests *Dictyostelium* IP_3-receptor-like protein as a possible mediator (Fig. 8). The link between intracellular calcium and cell speed is shown in our work and (Van Duijn and Van Haastert, 1992). Note that calcium pumping activities, which are essential to restore low cytosolic calcium concentrations, are omitted. (B,C) Protrusive and retractile activities of cell-substrate contact area as a function of cell speed. Data are gathered from Fig. 5 (Ax2 cells), Fig. 7 (LW6 and LW20 cells) and from data obtained with IP_3-receptor null cells (not shown). In B, the solid line is a linear least square fit of all data points (slope 9.2 µm; ordinate at origin 0.84 µm^2 second^{-1}). In C, solid and dotted lines are linear least square fits of protrusion and retraction frequencies (slope –0.03 and –0.02 µm^{-1}, respectively; ordinate at origin 0.13 and 0.09 Hz, respectively).

Journal of Cell Science

calcium blocker Gd^{3+} and the cell morphology changes and acceleration observed when the calcium concentration is raised under constant shear flow.

The calcium response of wild-type cells is however extremely slow, compared with the time expected for calcium diffusion within the cells. Furthermore, cells lacking the IP_3-receptor require 20 times more calcium to reach the same speed and respond even more slowly to external calcium changes. This suggests that in wild-type cells, the main calcium flux comes from internal stores and that external calcium entry stimulates internal calcium release, as observed in many cells. A possible candidate for this process is PLCδ, which is indeed activated by calcium in vegetative cells (Cubitt and Firtel, 1992). It has been shown in vitro that IP_3 triggers Ca^{2+} release from *Dictyostelium* intracellular compartments (Schaloske et al., 2000). In this way, intracellular calcium release would amplify the small calcium entry from the plasma membrane. Without IP_3-receptors, residual sensitivity to external calcium is however still possible, whereas it is abolished in Gβ-null cells. Heterotrimeric G proteins would control plasma membrane calcium channels in vegetative motile cells. A tentative scheme combining the biochemical knowledge of *Dictyostelium* signaling pathways and our new results is depicted in Fig. 9.

Using fluorescent markers, no gross change in cytoplasmic calcium concentration is experimentally observed. Calcium variations are indeed well buffered within *Dictyostelium* cells and therefore, calcium concentration changes are necessarily restricted to the border of plasma membrane or internal calcium stores. A localized calcium increase would facilitate the turnover of actin polymerization-depolymerization, for instance by activating proteins such as gelsolin, whose activity is modulated by calcium at a 15-25 μM affinity (Ditsch and Wegner, 1995; Kinosian et al., 1998). Calcium is therefore involved in the fast remodeling of actin structures rather than in cell polarization mechanisms.

A correlation between intracellular calcium levels and chemotactic motility has already been observed in neutrophils (Mandeville et al., 1995). Furthermore, internal calcium concentrations periodically fluctuate in moving keratocytes and application of shear stress by stretching a flexible substrate underneath the cell induces a calcium transient (Lee et al., 1999). Recently, it was reported that ultrafast Ca^{2+} waves travel through fMLP-stimulated neutrophils (Kindzelskii and Petty, 2003). In *Dictyostelium* cells, cAMP receptor activation stimulates calcium entry (Nebl et al., 2002; Schaloske et al., 2000; Yumura et al., 1996), but eliminating capacitive calcium entry by knocking out the *Dictyostelium* IP_3-receptor-like gene does not affect chemotaxis speed and directionality (Traynor et al., 2000). It should, however, be noted that in the reported cAMP chemotaxis experiments, *Dictyostelium* speed was close to that observed during random motility, suggesting that stimulation was not at its maximal. In addition, introduction of EGTA calcium buffer stops net cell movement but does not prevent cell orientation in the direction of a cAMP gradient, revealed by protrusion elongation in this direction (Unterweger and Schlatterer, 1995; Van Duijn and Van Haastert, 1992). Intracellular loading with BAPTA, a calcium buffer which has a similar Ca^{2+} dissociation constant to EGTA but an about 150-fold faster rate of Ca^{2+} binding (Tsien, 1980), prevents both motility and oriented pseudopod emission (Schlatterer and Malchow, 1993; Unterweger and Schlatterer, 1995). It seems, therefore, likely that during chemotaxis as well, calcium controls cell speed, but not directionality. At this stage of our knowledge, chemotaxis and shear-flow-induced motility signaling pathways differ in two respects. (1) Heterotrimeric G proteins are essential for cAMP and folic acid signal transduction but are dispensable for mechanosensitivity. (2) The phg2 kinase is required for vegetative cell explorative or shear-flow-induced motility but not during multicellular development, hence for cAMP chemotaxis (Gebbie et al., 2004).

The new image analysis procedure developed in this work points out to the existence of oscillations in the cell edge movement, at a 9 and 12 seconds period for protrusions and retractions, respectively. The amplitude of these oscillations increases with cell speed, but their frequency is almost constant. The linear relationship between gained or lost area growth rate and cell speed is easily interpreted. Some protrusions and retractions of the cell edge are effective since they result in net cell movement. Others do not and their activity is independent of cell speed. We can thus write the area growth rate as the sum of two terms:

$$\mathrm{d}A/\mathrm{d}t = (\mathrm{d}A/\mathrm{d}t)_0 + L \times v \,, \qquad (8)$$

where $(\mathrm{d}A/\mathrm{d}t)_0$ is the ineffective cell protrusive or retractive activity and L is a length, which relates cell speed to the growth rate of the cell-substrate contact area. This is the length along which gained or lost areas are in the direction of cell movement. In a perfectly aligned cell, L is the width of protrusions or retractions. It is noteworthy that all data obtained with all four cell lines used (Ax2, LW6, LW20 and IP_3-receptor null cells) can be put on the same graphs (Fig. 9B,C), giving $(\mathrm{d}A/\mathrm{d}t)_0$=0.84±0.14 μm^2 s^{-1} and L=9.2±0.7 μm under the reported RICM experimental conditions. $(\mathrm{d}A/\mathrm{d}t)_0$ is comparable with the smallest recorded peaks. L is about a quarter of the cell-substrate contact perimeter. This makes sense, because this is the typical length of the cell contour facing or opposite to the flow[‡]. Thus for wild-type cells, the protrusion and retraction activities become more and more effective as the calcium concentration increases. As for the peak frequencies, they slightly decrease with cell speed. The oscillation period, therefore, does not contribute significantly to cell speed changes.

Finally, this work extends our previous report of directional mechano-sensitivity: at low shear stress (0.5 Pa), cells tend to oppose to the force exerted by the flow whereas they tend to move in the direction of the force at higher shear stress. *Dictyostelium* indeed recapitulates the behavior of various cell lines: keratocytes, for instance, move in the direction of the force (Verkhovsky et al., 1999) in contrast to fibroblasts, which oppose detachment by reinforcing focal contacts (Riveline et al., 2001). It should be noted that at a shear stress giving rise to zero directionality (about 0.6-1.2 Pa), cell behavior is not random, but clearly bi-directional (see supplementary material, Movie 3). Bi-directionality of cell movement is indicative of a complex relationship between cell edge velocity and membrane tension. At each cell edge, two alternative macromolecular assemblies can indeed be recruited, that allow

[‡]Using all RICM recordings, we measured the average contact length between the gained and the steady areas L_1, and the average contact length between the lost and steady area L_2. L_1 and L_2 are independent of the external calcium concentration (data not shown) and indeed comparable to L: L_1=8.4±3.5 μm, L_2=9.5±4.1 μm.

spreading or retraction. These machineries are both mechanically and biochemically incompatible at the same site (Meili and Firtel, 2003; Xu et al., 2003). Our results show that membrane tension, which is modulated by shear-flow within a single cell, affects the state of the complex actin cytoskeleton dynamics.

This work was supported by the Commissariat à l'Energie Atomique, the Centre National de la Recherche Scientifique and the University Joseph Fourier. This work was also supported by a jointed grant 'Dynamique et Réactivité des Assemblages Moléculaires' from the Ministère de la Recherche and the Centre National de la Recherche Scientifique and a special grant from the Institut de la Matière Condensée (Grenoble). Bernard Sartor provided excellent technical assistance. We thank Jean-Marc Chaix (ENSEEG Grenoble) for advice about image analysis. F.C., J.D. and S.F. are recipients of a MENRT fellowship.

References

Bailly, M. and Condeelis, J. (2002). Cell motility: insights from the backstage. *Nat. Cell Biol.* **4**, 292-294.

Borisy, G. G. and Svitkina, T. M. (2000). Actin machinery: pushing the envelope. *Curr. Opin. Cell. Biol.* **12**, 104-112.

Carlier, M. F. and Pantaloni, D. (1997). Control of actin dynamics in cell motility. *J. Mol. Biol.* **269**, 459-467.

Chadwick, C. M., Ellison, J. E. and Garrod, D. R. (1984). Dual role for *Dictyostelium* contact site B in phagocytosis and developmental size regulation. *Nature* **307**, 646-647.

Clow, P. A. and McNally, J. G. (1999). In vivo observations of myosin II dynamics support a role in rear retraction. *Mol. Biol. Cell* **10**, 1309-1323.

Coates, J. C. and Harwood, A. J. (2001). Cell-cell adhesion and signal transduction during *Dictyostelium* development. *J. Cell Sci.* **114**, 4349-4358.

Cubitt, A. B. and Firtel, R. A. (1992). Characterization of phospholipase activity in Dictyostelium discoideum. Identification of a Ca(2+)-dependent polyphosphoinositide-specific phospholipase C. *Biochem. J.* **283**, 371-378.

Décavé, E., Garrivier, D., Brechet, Y., Fourcade, B. and Bruckert, F. (2002). Shear-flow-induced detachment kinetics of *Dictyostelium discoideum* cells from solid substrate. *Biophys. J.* **82**, 2383-2395.

Décavé, E., Rieu, D., Dalous, J., Fache, S., Brechet, Y., Fourcade, B., Satre, M. and Bruckert, F. (2003). Shear-flow-induced motility of Dictyostelium discoideum cells on solid substrate. *J. Cell Sci.* **116**, 4331-4343.

DesMarais, V., Ichetovkin, I., Condeelis, J. and Hitchcock-DeGregori, S. E. (2002). Spatial regulation of actin dynamics: a tropomyosin-free, actin rich compartment at the leading edge. *J. Cell Sci.* **115**, 4649-4660.

Devreotes, P. and Janetopoulos, C. (2003). Eukaryotic chemotaxis: distinctions between directional sensing and polarization. *J. Biol. Chem.* **278**, 8.

Ditsch, A. and Wegner, A. (1995). Two low-affinity Ca(2+)-binding sites of gelsolin that regulate association with actin. *Eur. J. Biochem.* **229**, 512-516.

Drayer, A. L., Van der Kaay, J., Mayr, G. W. and Van Haastert, P. J. (1994). Role of phospholipase C in Dictyostelium: formation of inositol 1,4,5-trisphosphate and normal development in cells lacking phospholipase C activity. *EMBO J.* **13**, 1601-1609.

Friedl, P., Borgmann, S. and Brocker, E. B. (2001). Amoeboid leukocyte crawling through extracellular matrix: lessons from the *Dictyostelium* paradigm of cell movement. *J. Leukocyte Biol.* **70**, 491-509.

Fukui, Y., Lynch, T. J., Brzeska, H. and Korn, E. D. (1989). Myosin I is located at the leading edges of locomoting Dictyostelium amoebae. *Nature* **341**, 328-331.

Gasteier, J. E., Madrid, R., Krautkramer, E., Schroder, S., Muranyi, W., Benichou, S. and Fackler, O. T. (2003). Activation of the Rac-binding partner FHOD1 induces actin stress fibers *via* a ROCK-dependent mechanism. *J. Biol. Chem.* **278**, 38902-38912.

Gebbie, L., Benghezal, M., Cornillon, S., Froquet, R., Cherix, N., Malbouyres, M., Lefkir, Y., Grangeasse, C., Fache, S., Dalous, J. et al. (2004). Phg2, a kinase involved in adhesion and focal site modeling in Dictyostelium. *Mol. Biol. Cell* **15**, 3915-3925.

Grimson, M. J., Coates, J. C., Reynolds, J. P., Shipman, M., Blanton, R. L. and Harwood, A. J. (2000). Adherens junctions and beta-catenin-mediated cell signalling in a non-metazoan organism. *Nature* **408**, 727-731.

Kindzelskii, A. L. and Petty, H. R. (2003). Intracellular calcium waves accompany neutrophil polarization, formylmethionylleucylphenylalanine stimulation, and phagocytosis: a high speed microscopy study. *J. Immunol.* **170**, 64-72.

Kinosian, H. J., Newman, J., Lincoln, B., Selden, L. A., Gershman, L. C. and Estes, J. E. (1998). Ca2+ regulation of gelsolin activity: binding and severing of F-actin. *Biophys. J.* **75**, 3101-3139.

Knecht, D. A., Fuller, D. L. and Loomis, W. F. (1987). Surface glycoprotein, gp24, involved in early adhesion of *Dictyostelium discoideum*. *Dev. Biol.* **121**, 277-283.

Krause, M., Dent, E. W., Bear, J. E., Loureiro, J. J. and Gertler, F. B. (2003). Ena/VASP proteins: regulators of the actin cytoskeleton and cell migration. *Annu. Rev. Cell Dev. Biol.* **19**, 541-564.

Lee, J., Ishihara, A., Oxford, G., Johnson, B. and Jacobson, K. (1999). Regulation of cell movement is mediated by stretch-activated calcium channels. *Nature* **400**, 382-386.

Lilly, P., Wu, L., Welker, D. L. and Devreotes, P. N. (1993). A G protein beta-subunit is essential for Dictyostelium development. *Genes Dev.* **7**, 986-995.

Lin, K. M., Wenegieme, E., Lu, P. J., Chen, C. S. and Yin, H. L. (1997). Gelsolin binding to phosphatidylinositol 4,5-bisphosphate is modulated by calcium and pH. *J. Biol. Chem.* **272**, 50.

Mandeville, J. T., Ghosh, R. N. and Maxfield, F. R. (1995). Intracellular calcium levels correlate with speed and persistent forward motion in migrating neutrophils. *Biophys. J.* **68**, 1207-1217.

Meili, R. and Firtel, R. A. (2003). Two poles and a compass. *Cell* **114**, 153-156.

Nebl, T. and Fisher, P. R. (1997). Intracellular Ca2+ signals in Dictyostelium chemotaxis are mediated exclusively by Ca2+ influx. *J. Cell Sci.* **110**, 2845-2853.

Nebl, T., Kotsifas, M., Schaap, P. and Fisher, P. R. (2002). Multiple signalling pathways connect chemoattractant receptors and calcium-channels in Dictyostelium. *J. Muscle Res. Cell Motil.* **23**, 853-865.

Niewohner, J., Weber, I., Maniak, M., Muller-Taubenberger, A. and Gerisch, G. (1997). Talin-null cells of *Dictyostelium* are strongly defective in adhesion to particle and substrate surfaces and slightly impaired in cytokinesis. *J. Cell Biol.* **138**, 349-361.

Pollard, T. D. and Borisy, G. G. (2003). Cellular motility driven by assembly and disassembly of actin filaments. *Cell* **112**, 453-465.

Riveline, D., Zamir, E., Balaban, N. Q., Schwarz, U. S., Ishizaki, T., Narumiya, S., Kam, Z., Geiger, B. and Bershadsky, A. D. (2001). Focal contacts as mechanosensors: externally applied local mechanical force induces growth of focal contacts by an mDia1-dependent and ROCK-independent mechanism. *J. Cell Biol.* **153**, 1175-1186.

Rooney, E. K., Gross, J. D. and Satre, M. (1994). Characterisation of an intracellular Ca2+ pump in Dictyostelium. *Cell Calcium* **16**, 509-522.

Sakisaka, T., Itoh, T., Miura, K. and Takenawa, T. (1997). Phosphatidylinositol 4,5-bisphosphate phosphatase regulates the rearrangement of actin filaments. *Mol. Cell Biol.* **17**, 3841-3849.

Schaloske, R., Schlatterer, C. and Malchow, D. (2000). A Xestospongin C-sensitive Ca(2+) store is required for cAMP-induced Ca(2+) influx and cAMP oscillations in Dictyostelium. *J. Biol. Chem.* **275**, 8404-8408.

Schlatterer, C. and Malchow, D. (1993). Intracellular Gunaosine-5′-O-(3-thiotriphosphate) blocks chemotactic motility of Dictyostelium discoideum amoebae. *Cell Motil. Cytoskeleton* **25**, 298-307.

Traynor, D., Milne, J. L., Insall, R. H. and Kay, R. R. (2000). Ca(2+) signalling is not required for chemotaxis in Dictyostelium. *EMBO J.* **19**, 4846-4854.

Tsien, R. Y. (1980). New calcium indicators with high selectivity against magnesium and protons: design, synthesis, and properties of prototype structures. *Biochemistry* **19**, 2396-2404.

Unterweger, N. and Schlatterer, C. (1995). Introduction of calcium buffers into the cytosol of Dictyostelium discoideum amoebae alters cell morphology and inhibits chemotaxis. *Cell Calcium* **17**, 97-110.

Van Duijn, B. and Van Haastert, P. J. (1992). Independent control of locomotion and orientation during Dictyostelium discoideum chemotaxis. *J. Cell Sci.* **102**, 763-768.

Verkhovsky, A. B., Svitkina, T. M. and Borisy, G. G. (1999). Self-polarization and directional motility of cytoplasm. *Curr. Biol.* **9**, 11-20.

Watts, D. J. and Ashworth, J. M. (1970). Growth of myxameobae of the cellular slime mould Dictyostelium discoideum in axenic culture. *Biochem. J.* **119**, 171-174.

Welch, M. D. and Mullins, R. D. (2002). Cellular control of actin nucleation. *Annu. Rev. Cell Dev. Biol.* **18**, 247-288.

Wolven, A. K., Belmont, L. D., Mahoney, N. M., Almo, S. C. and Drubin, D. G. (2000). In vivo importance of actin nucleotide exchange catalyzed by profilin. *J. Cell Biol.* **150**, 895-904.

Wong, E. F., Brar, S. K., Sesaki, H., Yang, C. and Siu, C. H. (1996). Molecular cloning and characterization of DdCAD-1, a Ca2+-dependent cell-cell adhesion molecule, in *Dictyostelium discoideum*. *J. Biol. Chem.* **271**, 16399-16408.

Wu, L., Valkema, R., Van Haastert, P. J. and Devreotes, P. N. (1995). The G protein beta subunit is essential for multiple responses to chemoattractants in Dictyostelium. *J. Cell Biol.* **129**, 1667-1675.

Xu, J., Wang, F., Van Keymeulen, A., Herzmark, P., Straight, A., Kelly, K., Takuwa, Y., Sugimoto, N., Mitchison, T. and Bourne, H. R. (2003). Divergent signals and cytoskeletal assemblies regulate self-organizing polarity in neutrophils. *Cell* **114**, 201-214.

Yumura, S., Furuya, K. and Takeuchi, I. (1996). Intracellular free calcium responses during chemotaxis of Dictyostelium cells. *J. Cell Sci.* **109**, 2673-2678.

Journal of Cell Science

Journal of Cell Science

Journal of Cell Science 118, 3445-3457 Published by The Company of Biologists 2005
doi:10.1242/jcs.02461

Supplementary Material

Table S1. Ionic composition of the bathing fluid and SFICM

Ax2 cells were introduced in the shear flow chamber in Sörensen buffer, then the buffer was exchanged for the indicated ones at low shear stress and after 3 min, high shear stress was applied (σ = 2.4 Pa). SFICM was recorded and measured as explained in Materials and Methods. The first four solutions test for the involvement of Na^+, K^+, Ca^{2+} and Mg^{2+} in SFICM. The last fours show that H^+ marginally influences SFICM. It should be noted that cells detach from the surface at pH larger than 7.5.

Bathing solution	Speed (μm/min)	Directionality
20 mM MES-NaOH, pH 6.5	10 ± 2	0.8 ± 0.1
20 mM MES-KOH, pH 6.5	10.3 ± 0.8	0.7 ± 0.1
20 mM MES-NaOH, pH 6.5 + 1 mM $CaCl_2$	26 ± 2	0.9 ± 0.1
20 mM MES-NaOH, pH 6.5 + 1 mM $MgCl_2$	10 ± 2	0.8 ± 0.1
20 mM MES-NaOH, pH 5.0	3.5 ± 0.5	0.7 ± 0.2
20 mM MES-NaOH, pH 5.5	4.7 ± 0.7	0.8 ± 0.1
20 mM MES-NaOH, pH 6.0	10 ± 2	0.8 ± 0.1
20 mM MES-NaOH, pH 7.0	10 ± 2	0.8 ± 0.1